P_{AOX1} expression in mixed-substrate continuous cultures of *Komagataella phaffii* (*Pichia pastoris*) is completely determined by methanol uptake regardless of the secondary carbon source: a simplifying principle for predicting recombinant protein production

Running title: P_{AOX1} expression is completely determined by methanol uptake

Anamika Singh and Atul Narang*

Department of Biochemical Engineering and Biotechnology, Indian Institute of Technology, Hauz Khas, New Delhi 110016, India

Email: anarang@dbeb.iitd.ac.in

Telephone: +91-11-2659-1061

Funding Information: This research was supported by the grant BT/PR13831/BBE/117/68/2015 received from the Department of Biotechnology (DBT), Government of India.

Abstract

The expression of recombinant proteins by the AOX1 promoter of *Komagataella phaffii* is typically induced by adding methanol to the cultivation medium. Since growth on methanol imposes a high oxygen demand, the medium is often supplemented with an additional "secondary" carbon source which serves to reduce the consumption of methanol, and hence, oxygen. Early research recommended the use of glycerol as the secondary carbon source, but more recent studies recommend the use of sorbitol because glycerol represses P_{AOX1} expression. To assess the validity of this recommendation, we measured the steady state concentrations of biomass, residual methanol, and AOX1 over a wide range of dilution rates (0.02–0.20 h^{-1}) in continuous cultures of the Mut^+ strain fed with methanol, methanol + glycerol, and methanol + sorbitol. We find that when the specific AOX1 expression and methanol uptake rates for each of the three feeds are plotted against each other, they collapse into a single hyperbolic curve. The specific AOX1 expression rate is therefore completely determined by the specific methanol uptake rate regardless of the existence (present/absent) and type (repressing/non-repressing) of the secondary carbon source. In particular, cultures fed with methanol + glycerol and methanol + sorbitol that consume methanol at equal rates also express the protein at equal rates and levels. Now, it turns out that the simple unstructured model developed by Egli and co-workers can predict the specific methanol uptake rates of single- and mixed-substrate cultures over a wide range of dilution rates and feed concentrations. By combining this model with our data, we derive simple formulas that predicts the protein expression rates and levels of single- and mixed-substrate cultures over a wide range of conditions.

1. Introduction

The methylotrophic yeast *Komagataella phaffii,* referred to earlier as *Pichia pastoris* (Kurtzman, 2005; Kurtzman, 2009), is a popular expression host (Schwarzhans *et al*., 2016). There are several reasons for this, but the most important one is that *K. phaffii* has an unusually strong and tightly regulated promoter which drives the expression of alcohol oxidase (AOX) in the presence of methanol (Higgins and Cregg, 1998; Ahmad *et al.*, 2014; Gasser and Mattanovich, 2018). To be sure, *K. phaffii* has two alcohol oxidase genes, *AOX1* and *AOX2*, with corresponding promoters, P_{AOX1} and P_{AOX2}, but P_{AOX1} is used to drive recombinant protein expression since it is ~10 times stronger than P_{AOX2} (Cregg *et al.*, 1989).

In the first expression system constructed with *K. phaffii*, the wild-type strain was used as host, and recombinant protein was expressed under the control of P_{AOX1} by using methanol as inducer (Cregg *et al*., 1985). Although this Mut^+ (methanol utilization plus) strain yielded excellent recombinant protein expression, the use of methanol as inducer led to several operational problems (McCauley-Patrick *et al.,* 2005; Cos *et al.,* 2006; Jahic *et al.,* 2006; Jungo *et al.,* 2007a; Arnau *et al.,* 2011; Potvin *et al.,* 2012; Yang and Zhang, 2018; Garcia-Ortega *et al.,* 2019; Liu *et al.,* 2019). Indeed, methanol is inflammable which poses safety issues. Moreover, methanol metabolism results in high oxygen demand and heat generation, as well as excretion of toxic metabolites such as formaldehyde that inhibit growth (Jungo *et al*., 2007b; Juturu and Wu, 2018).

The problems stemming from the use of methanol as inducer have led to several strategies for reducing methanol uptake. One such strategy was to engineer the host strain by deleting either *AOX1* or both *AOX1* and *AOX2*, thus producing the Mut^S (methanol utilization slow) and Mut^- (methanol utilization minus) strains, respectively, whose capacity to consume methanol is substantially impaired or abolished (Chiruvolu *et al*., 1997). Another strategy was to introduce into the medium, in addition to the *primary* or *inducing* carbon source methanol, a *secondary* or *non-inducing* carbon source that supports growth but not induction. This reduces methanol consumption due to the sparing effect of the secondary carbon source, and increases the volumetric productivity due to the enhanced cell density derived from metabolism of the secondary carbon source (Brierley *et al*., 1990; Jungo *et al*., 2007a; Jungo *et al*., 2007b; Paulova et al., 2012).

The foregoing strategies have led to reduced methanol consumption, but they can also result in decreased recombinant protein expression. Recently, we found that host strain engineering decreases recombinant protein expression substantially — the specific productivities of the engineered Mut^S and Mut^- strains are respectively 5- and 10-fold lower than that of the Mut^+ strain (Singh and Narang, 2020). Since these three strains differ only with respect to their capacity for methanol uptake, it is clear that the methanol uptake rate is an important determinant of the P_{AOX1} expression rate.

The goal of this work is to quantify the extent to which P_{AOX1} expression is affected by addition of a secondary carbon source to the medium. It is commonly held that this is determined by the type of the secondary carbon source. Specifically, these carbon sources have been classified as *repressing* or *non-repressing* based on the P_{AOX1} expression levels observed in batch cultures of the Mut^- strain grown on mixtures of methanol and various secondary carbon sources (Inan and Meagher, 2001). Repressing carbon sources, such as glycerol, abolish P_{AOX1} expression, whereas non-repressing carbon sources, such as sorbitol, permit P_{AOX1} expression. The same conclusion has been reached from studies of mixed-substrate growth in fed-batch cultures (Brierley *et al*., 1990; Thorpe *et al*., 1999; Xie *et al*., 2005; Çelik *et al.,* 2009; Wang *et al.,* 2010; Gat *et al.,* 2012; Niu *et al.,* 2013; Carly *et al.,* 2016; Azadi *et al.,* 2017; Chen *et al.,* 2017) and continuous cultures (Jungo *et al.,* 2006; Jungo *et al*., 2007a; Jungo *et al*., 2007b; Canales *et al*., 2015; Berrios *et al*., 2016). Indeed, even though glycerol is the most commonly used secondary carbon source, the use of sorbitol has been almost unanimously recommended on the grounds that glycerol represses P_{AOX1} expression.

Most of the comparative studies cited above used constant fed-batch cultures, but these data can be difficult to interpret physiologically because the specific growth rate decreases throughout the course of the experiment (Nieto-Taype *et al.,* 2020). The comparative studies with continuous cultures are reviewed at length in the Discussion. Here, it suffices to note that many of these studies were performed at a fixed dilution rate D, and hence, specific growth rate (Jungo *et al*., 2007a; Jungo *et al*., 2007b; Berrios *et al*., 2016). We reasoned that comparative studies over a wide range of D could yield deeper physiological insights into the factors governing P_{AOX1} expression. Moreover, the optimal operating conditions determined in continuous cultures can also inform optimal protein production in exponential fed-batch cultures (Jungo *et al*., 2007a; Jungo *et al*., 2007b).

We were therefore led to study P_{AOX1} expression in continuous cultures of *K. phaffii* fed with fixed concentrations of methanol, methanol + glycerol, and methanol + sorbitol, and operated at various D. To this end, we used a Mut$^+$ strain which expressed LacZ from P_{AOX1}, but to enable consistency checks, we also measured the AOX expressed from the native AOX1 promoter. We find that the specific AOX1 expression rate is completely determined by the specific methanol uptake rate regardless of the existence (present/absent) and type (repressing/non-repressing) of the secondary carbon source. This result enables us to provide simple formulas that predict the specific activity and productivity of recombinant proteins over a wide range of operating conditions.

2. Materials and Methods:

2.1 Microorganism and growth medium

A *K. phaffii* Mut$^+$ strain, GS115 (*his4*) was procured from J. M. Cregg, Keck Graduate Institute, Claremont, CA, USA and was genetically modified to express a recombinant β-galactosidase protein. Details of the strain construction have been presented elsewhere (Singh and Narang, 2020). The resulting strain was called Mut$^+$ (pSAOH5-T1) and was used for this study. Stock cultures were stored in 25% glycerol at –80 °C.

The minimal medium composition used for shake-flask as well as chemostat cultivations was chosen such as to prevent any stoichiometric limitation with respect to the carbon source as described in Egli and Fiechter (1981). The defined medium was supplemented with either glycerol, methanol or a mixture of methanol and glycerol/sorbitol as carbon sources and in addition, contained 100 mM phosphate buffer (pH 5.5), 15.26 g NH_4Cl, 1.18 g $MgSO_4.7H_2O$, 110 mg $CaCl_2.2H_2O$, 45.61 mg $FeCl_3$, 28 mg $MnSO_4.H_2O$, 44 mg $ZnSO_4.7H_2O$, 8 mg $CuSO_4.5H_2O$, 8.57 mg $CoCl_2.6H_2O$, 6 mg $Na_2MoO_4.2H_2O$, 8 mg H_3BO_3, 1.2 mg KI, 370 mg EDTA disodium salt, 2.4 mg biotin per liter. All components of the defined medium were prepared and sterilised by either filtration or autoclaving as separate stock solutions and then mixed before cultivation.

2.2 Inoculum preparation and chemostat cultivation

When required, cells were revived in a 100 mL shake flask containing 10 mL minimal medium supplemented with a suitable carbon source at 30 °C. These primary cultures were sub-

cultured once before inoculating the reactor precultures (in the same cultivation medium as prepared for the reactor vessel) which were then used as an inoculum for the bioreactor.

Chemostat cultivations were performed using bench-scale 0.5 L mini bioreactors modified to support chemostat operation and equipped with pH, DO, temperature, level and agitation controls (Applikon Biotechnology, The Netherlands) with working volumes of 0.3 L. The cultivation temperature was always maintained at 30 °C and pH at 5.5 by the automatic addition of 2 M NaOH. An integrated mass flow controller ensured a constant supply of air to the reactor vessel at 80 mL min^{-1}. Dissolved oxygen levels were monitored by a polarographic probe calibrated with respect to an air-saturated medium. Cultures were agitated to ensure aerobic conditions (DO level was maintained above 60 % saturation at all times) and fast mixing of the feed. An anti-foam agent was added to the reactor vessel as and when required to prevent foam formation and wall growth. For chemostat mode operation, the dilution rate was set by fixing the input feed flow rate while a constant volume was maintained inside the reactor vessel by controlling the output feed flow rate via proportional control based on the on-line monitoring of the change in weight of the reactor vessel. The O_2 and CO_2 levels in the off-gas were measured using a Tandem gas analyser (Magellan Biotech, UK). After inoculation, cells were grown in batch phase for some time to allow exhaustion of the initial carbon source (indicated by a rise in DO level), followed by initiating the input and output feed supplies. At any particular dilution rate, steady-state samples were withdrawn after 5-6 liquid residence times. In general, three samples were collected for each dilution rate, separated by an interval of one liquid residence time.

2.3 Sample collection and processing

For determination of residual substrate concentration inside the reactor, samples were withdrawn directly from the vessel. To achieve rapid biomass separation, culture samples were withdrawn using vacuum through a sampling tube attached to a 0.2-micron syringe filter and stored at –20 °C until analysis. Samples for determination of biomass and specific enzyme activities were collected in a sampling bottle kept on ice. Biomass samples were processed immediately, while samples for measuring enzyme activities were pelleted, washed and stored at –20 °C until processing.

2.4 Substrate analysis

Glycerol and sorbitol concentrations were estimated by high-performance liquid chromatography (HPLC) analysis (1100 series, Agilent Technologies, Palo Alto, USA). An ion-exclusion chromatography column from Phenomenex, California, USA (ROA-Organic acid H^+ column, 300 x 7.8 mm, 8 µm particle size, 8% cross linkage) with a guard column (Carbo-H cartridges) was used with 5 mM H_2SO_4 in ultrapure water as mobile phase supplied at a constant flow rate of 0.5 mL min^{-1}. The column chamber was maintained at 60 °C and a refractive index detector was used for substrate measurement. Methanol concentrations were determined with a gas chromatograph equipped with a flame ionisation detector (GC-FID) (7890A, Agilent Technologies, Palo Alto, USA) using a HP-PLOT/Q column (30 m x 0.32 mm, 20 µm) from Agilent Technologies and nitrogen as the carrier gas.

2.5 Dry cell weight measurement

A known volume of the fermentation broth was collected and pelleted in a pre-weighed centrifuge tube. Pellets were washed twice with distilled water and then dried at 80 °C to constant weight.

2.6 Cell-free extract preparation

Culture samples were collected on ice and immediately centrifuged at 4 °C to collect cells. The cell pellets were washed twice with phosphate buffer (100 mM, pH 7.4) and stored at –20 °C until analysis. For cell lysis, pellets were resuspended in 100 µl of chilled breaking buffer (Jungo *et al*., 2006). Acid-washed glass beads (0.40–0.45 mm diameter) were added to the resulting slurry followed by alternate vortexing (1 min) and resting (on ice for 1 min) steps. This cycle was repeated 4-5 times, after which the cell debris was removed by centrifugation. Cell-free extracts (supernatant) were collected in fresh tubes kept on ice and immediately used for the estimation of enzyme activities. The Bradford assay was used for the estimation of the total protein content of the cell-free extracts for which bovine serum albumin served as standard.

2.7 β-galactosidase assay

β-galactosidase assays were performed according to the method described by Miller (1972) with modifications. Briefly, cell-free extracts were appropriately diluted and mixed with Z-buffer containing β-mercaptoethanol (Miller 1972) and incubated at 30 °C in a water-bath for

15-20 minutes. The reaction was started by adding ONPG and stopped by adding Na_2CO_3 when sufficient colour had developed. The specific β-galactosidase activity was calculated with the formula

$$1000 \times \frac{\mathrm{OD}_{420}/\text{Reaction time (min)}}{\text{Protein concentration in extract (mg/mL)} \times \text{Sample volume (mL)}}$$

and expressed in units mgp^{-1} where mgp denotes mg of total protein.

2.8 Alcohol oxidase assay

Appropriate dilutions of the cell-free extracts were used to measure alcohol oxidase activities based on the method adapted from Jungo et al (2006). A fresh 2x stock of the assay reaction mixture containing 0.8 mM 4-aminoantipyrine, 50 mM phenolsulfonic acid, freshly prepared 4 U/mL horseradish peroxidase in potassium phosphate buffer (200 mM, pH 7.4) was prepared before setting up the assays. 100 µL of the diluted cell-free extracts were mixed with 25 µL methanol and incubated at 30 °C for 10 minutes. After this, 100 µL of the 2x reaction mixture stock was added to the mix at time t = 0 to start the reaction and the increase in absorbance at 500 nm was monitored every 30 seconds for 10 minutes using a microplate reader (SpectraMax M2e, Molecular Devices Corporation, CA, USA). The specific alcohol oxidase activity was calculated with the formula

$$100{,}000 \times \frac{\mathrm{OD}_{500}/\text{Reaction time (s)}}{\text{Protein concentration in extract (mg/mL)} \times \text{Sample volume (mL)}}$$

and reported in units mgp^{-1}.

2.9 Calculating substrate consumption and protein expression rates from the data

We are concerned with experiments in which a chemostat is fed with the primary carbon source S_1 (methanol), or a mixture of S_1 and a secondary carbon source S_2 which may be repressing (glycerol) or non-repressing (sorbitol). The primary carbon source S_1 induces the synthesis of the enzyme E_1 which represents AOX and LacZ since both enzymes are expressed from the *AOX1* promoter. We are interested in the steady state concentrations of biomass X, primary carbon source S_1, secondary carbon source S_2, and enzyme E_1, which are denoted x, s_1, s_2, and e_1 respectively, and satisfy the mass balances:

$$0 = \frac{dx}{dt} = -Dx + \mu x, \qquad (1)$$

$$0 = \frac{ds_1}{dt} = D\left(s_{f,1} - s_1\right) - r_{s,1}x, \tag{2}$$

$$0 = \frac{ds_2}{dt} = D\left(s_{f,2} - s_2\right) - r_{s,2}x, \tag{3}$$

$$0 = \frac{de_1}{dt} = r_{e,1} - \mu e_1, \tag{4}$$

where $s_{f,1}$, $s_{f,2}$ denote the feed concentrations of S_1, S_2, respectively, and μ, $r_{s,1}$, $r_{s,2}$, $r_{e,1}$ denote the specific rates of growth, substrate consumption and enzyme expression, respectively. It follows from Eqs. (1)–(4) that

$$r_{s,i} = \frac{D(s_{f,i} - s_i)}{x}, i = 1,2, \tag{5}$$

$$r_{e,1} = De_1. \tag{6}$$

These equations were used to calculate $r_{s,1}$, $r_{s,2}$, and $r_{e,1}$ from the measured values of the operating conditions D, $s_{f,i}$ and the steady state concentrations s_i, x, and e_1.

2.10 Predicting the biomass concentration and substrate consumption rates

During single-substrate growth at sufficiently low D, the biomass concentrations and substrate consumption rates can be predicted from the biomass yield and operating conditions. Indeed, if Y_i denotes the single-substrate biomass yield of S_i, i.e., the fraction of S_i converted to biomass during single-substrate growth on S_i — which is constant at all operating conditions except the vanishingly small D at which maintenance is significant — then $\mu = Y_i r_{s,i}$. Substituting this relation in Eq. (1) and then adding Eq. (1) to Y_1 times Eq. (2) or Y_2 times Eq. (3) yields

$$x = Y_i\left(s_{f,i} - s_i\right), \tag{7}$$

which can be substituted in (5) to get

$$r_{s,i} = \frac{D}{Y_i}. \tag{8}$$

At sufficiently small D, the substrate entering the chemostat is almost completely consumed ($s_i \ll s_{f,i}$), so that $x \approx Y_i s_{f,i}$ and $r_{s,i} = D/Y_i$ are completely determined by the biomass yield and the operating conditions. In particular, $r_{s,i}$ depends on D, but is independent of the feed concentration $s_{f,i}$.

Egli and co-workers have shown that analogous expressions predict the biomass concentrations and specific substrate consumption rates in mixed-substrate cultures growing at sufficiently low D (Egli *et al.*, 1982; Egli *et al.*, 1986; Lendenmann *et al.*, 1996). Specifically, they showed that the biomass yield of a substrate during mixed-substrate growth is no different from its biomass yield during single-substrate growth. Hence, the specific growth rate of mixed-substrate cultures is well-approximated by the equation $\mu = Y_1 r_{s,1} + Y_2 r_{s,2}$. Substituting this relation in Eq. (1) and then adding Eq. (1) to Y_1 times Eq. (2) plus Y_2 times Eq. (3) yields

$$x = Y_1\left(s_{f,1} - s_1\right) + Y_2\left(s_{f,2} - s_2\right), \tag{9}$$

which can be substituted in (5) to obtain

$$r_{s,i} = \frac{D(s_{f,i} - s_i)}{Y_1\left(s_{f,1} - s_1\right) + Y_2\left(s_{f,2} - s_2\right)}. \tag{10}$$

At the low D corresponding to the dual-limited regime (Fig. S1a) both substrates are completely consumed, so that

$$x \approx Y_1 s_{f,1} + Y_2 s_{f,2}, \tag{11}$$

and

$$r_{s,i} \approx \frac{D s_{f,i}}{Y_1 s_{f,1} + Y_2 s_{f,2}} = \frac{D\sigma_i}{Y_1\sigma_1 + Y_2\sigma_2}, \tag{12}$$

where $\sigma_i \stackrel{\text{def}}{=} s_{f,i}/\left(s_{f,1} + s_{f,2}\right)$ is the fraction of S_i in the feed. Thus, even in mixed-substrate cultures growing at sufficiently low D, x and $r_{s,i}$ are completely determined by the single-substrate biomass yields and operating conditions. In particular, $r_{s,i}$ depends on D and σ_i, but is independent of the total feed concentration $s_{f,1} + s_{f,2}$.

It is convenient to rewrite Eqs. (10) and (12) in a form that reveals the relative magnitudes of $r_{s,i}$ during single- and mixed-substrate growth (Noel and Narang, 2009). To this end, rewrite (10) as

$$r_{s,i} = \left(\frac{D}{Y_i}\right)\beta_i \tag{13}$$

where

$$\beta_i \stackrel{\text{def}}{=} \frac{Y_i\left(s_{f,i} - s_i\right)}{Y_1\left(s_{f,1} - s_1\right) + Y_2\left(s_{f,2} - s_2\right)}$$

is the fraction of biomass derived from S_i. It follows that at every D, the specific substrate uptake rate of S_i in mixed-substrate cultures is proportional to that of single-substrate cultures, D/Y_i, with the proportionality constant $\beta_i < 1$. Now, in the dual-limited regime

$$\beta_i \approx \frac{Y_i\sigma_i}{Y_1\sigma_1 + Y_2\sigma_2} \qquad (14)$$

is an increasing function of σ_i with $\beta_i(0) = 0$ and $\beta_i(1) = 1$; it is also independent of D beyond the vanishingly small D at which maintenance is significant. Therefore, under this condition, $r_{s,i}$ is not only proportional to D/Y_i, but the proportionality constant β_i is an increasing function of σ_i that can be changed at will by a suitable choice of σ_i.

3. Results

3.1 Substrate consumption and P_{AOX1} expression in the presence of glycerol and sorbitol

Our goal is to study the growth and expression kinetics in the presence of methanol; however, for reasons given below, it is useful to also characterize these kinetics during single-substrate growth on the secondary carbon sources, glycerol and sorbitol. In batch (shake-flask) cultures grown on glycerol and sorbitol, the biomass yields were quite similar (~0.6 gdw g^{-1}), but the maximum specific growth rates μ_{m} were dramatically different (Table 1). Due to the exceptionally small μ_m of 0.03 h^{-1} on sorbitol, we could not perform chemostat experiments with pure sorbitol, but we did perform such experiments with glycerol. We found that the biomass and residual glycerol concentrations followed the pattern characteristic of single-substrate growth in continuous cultures (Fig. 1a). The specific glycerol uptake rate, calculated from these data using Eq. (5), increased linearly with D with a significant positive *y*-intercept (Fig. 1b). Fitting these data to Pirt's model (Pirt, 1965) gave a true biomass yield of 0.67 gdw g^{-1}, and specific maintenance rate of 0.07 g $gdw^{-1}h^{-1}$. The specific LacZ and AOX activities were proportional to each other, and decreased inversely with D for $D \lesssim 0.13$ h^{-1} (Fig. 1c). Hence, under this condition, the specific LacZ and AOX expression rates, which were calculated from these data using Eq. (6), are independent of D (Fig. 1d).

3.2 Substrate consumption and P_{AOX1} expression in the presence of pure methanol

In batch cultures of methanol, the maximum specific growth rate was 0.11 h^{-1} and the biomass yield was 0.29 g gdw^{-1} (Table 1). In continuous cultures fed with ~3.2 g l^{-1} of methanol, the biomass and residual methanol concentrations varies with D in a manner similar to that observed with glycerol (Fig. 2a). The specific methanol uptake rate calculated from these data also increases linearly with D, but the *y*-intercept, and hence the specific maintenance rate, is negligibly small (Fig. 2b). The biomass yield calculated from the slope of this plot (0.27 gdw g^{-1}) agrees with that obtained from batch cultures. The specific LacZ and AOX activities are constant up to $D = 0.04$ h^{-1}, and decrease inversely with D thereafter (Fig. 2c). Then it follows from Eq. (6) that the specific LacZ and AOX expression rates increase linearly up to $D = 0.04$ h^{-1}, and are constant thereafter (Fig. 2d). Thus, the specific P_{AOX1} expression rate saturates at its maximum value when D exceeds the *threshold dilution rate* of 0.04 h^{-1}. Under this condition, the specific methanol uptake rate exceeds 0.15 g gdw^{-1} h^{-1} (Fig. 2b), which can therefore be viewed as the *threshold specific methanol uptake rate* beyond which P_{AOX1} expression saturates at its maximum value.

3.3 Substrate consumption and P_{AOX1} expression in the presence of mixtures

When the Mut^+ strain is grown in batch cultures of methanol + glycerol and methanol + sorbitol, there is diauxic growth, but methanol is the *unpreferred* substrate during growth on methanol + glycerol, and the *preferred* substrate during growth on methanol + sorbitol (Ramón *et al.,* 2007). Such mixtures, which display diauxic growth in batch cultures, exhibit a characteristic substrate concentration profile in continuous cultures (Fig. S1a). In the *dual-limited* regime, which extends up to dilution rates approximately equal to the μ_m for the unpreferred substrate, both substrates limit growth because their residual concentrations s_i are on the order of their saturation constants $K_{s,i}$ ($s_i \sim K_{s,i}$), and therefore, both substrates are completely consumed ($s_i \ll s_{f,i}$). Beyond the dual-limited regime, only the preferred substrate limits growth because the residual concentration of the unpreferred substrate is well above its saturation constant. At the intermediate D corresponding to the *transition* regime, the preferred substrate is still consumed completely, but the unpreferred substrate is only partially consumed. Beyond the transition regime, the unpreferred substrate is not consumed at all.

When methanol + glycerol and methanol + sorbitol were fed to a continuous culture, the variation of the substrate concentrations with D was consistent with the characteristic pattern described above. In the dual-limited regime, both substrates were completely consumed — up to $D \approx \mu_m|_{\text{methanol}} = 0.11$ h^{-1} in Fig. 3a and $D \approx \mu_m|_{\text{sorbitol}} = 0.03$ h^{-1} in Fig. 4a. In the transition regime, the unpreferred substrate was partially consumed up to dilution rates well above its μ_m — up to $D = 0.2 \approx 2 \times \mu_m|_{\text{methanol}}$ h^{-1} in Fig. 3a, and up to $D = 0.08 \approx 3 \times \mu_m|_{\text{sorbitol}}$ h^{-1} in Fig. 4a.

The biomass concentrations in both mixtures were consistent with Egli's model described in Materials & Methods. More precisely, the biomass concentrations calculated using Eq. (11) were almost always within 20 % of the observed biomass concentrations (Fig. S2).

During single-substrate growth, the specific substrate consumption rate increases linearly with D up to washout, but during mixed-substrate growth, the specific substrate consumption rates increase linearly with D only in the dual-limited regime (Fig. S1b). The dashed lines in Figs. 3b and 4b show that the specific methanol uptake rates in the dual-limited regime are well-approximated by Eqs. (13)–(14). Beyond the dual-limited regime, the specific substrate uptake rates depart from linearity (Fig. S1b). In the case of methanol + glycerol, the specific methanol uptake rate decreases due to repression of methanol uptake by glycerol (Fig. 3b); in the case of methanol + sorbitol, the specific methanol uptake rate increases faster than linearly due to the enhanced methanol uptake that occurs in response to repression of sorbitol uptake by methanol (Fig. 4b). Although the specific methanol consumption rate vs D curves for methanol + glycerol and methanol + sorbitol have different shapes, they always remain below the specific methanol consumption rate vs D curve for pure methanol, which is consistent with Eq. (13). The abovementioned properties of methanol uptake will play a crucial role in our explanation of the P_{AOX1} expression kinetics.

Although glycerol is repressing and sorbitol is non-repressing, the specific LacZ and AOX activities on the two mixtures are essentially identical (Figs. 3c and 4c), a striking result to which we shall return later. Here, it suffices to observe that these specific activities are also qualitatively similar to those observed with pure methanol insofar as they are constant up to $D \approx 0.06$ h^{-1}, and decrease inversely with D thereafter. Hence, Eq. (6) implies that the specific LacZ and AOX expression rates increase linearly up to $D \approx 0.06$ h^{-1} and are constant thereafter (Figs. 3d and 4d). The specific P_{AOX1} expression rates of both mixtures therefore

saturate beyond the threshold dilution rate of $D \approx 0.06$ h^{-1}, which is higher than the threshold dilution rate of 0.04 h^{-1} for pure methanol. However, the specific methanol uptake rate of the mixtures at $D \approx 0.06$ h^{-1} is 0.15 g gdw^{-1} h^{-1} (Figs. 3b and 4b), which is the same as the specific methanol uptake rate on methanol at $D = 0.04$ h^{-1}. In other words, even though the single- and mixed-substrate cultures have different threshold dilution rates (0.04 and 0.06 h^{-1} , respectively), they have the same threshold specific methanol uptake rate (0.15 g gdw^{-1} h^{-1}), which we denote by $r_{s,1}^*$. Moreover, the maximum P_{AOX1} expression rates on the two mixtures are essentially identical (Figs. 3d and 4d), and similar to the one attained with pure methanol (Fig. 2d). Taken together, these data show that the single- and mixed-substrate cultures yield the same maximum specific P_{AOX1} expression rate — henceforth denoted $V_{e,1}$ — whenever the specific methanol uptake rate exceeds the unique threshold specific methanol uptake rate $r_{s,1}^*$.

To see why the threshold specific methanol uptake rate is attained at different dilution rates in single- and mixed-substrate cultures, let D^* denote the threshold dilution rate, i.e., the dilution rate at which the specific methanol uptake rate equals $r_{s,1}^*$. Then D^* for mixed-substrate cultures is higher than the D^* for pure methanol simply because at every D, the specific methanol uptake rate of mixed-substrate cultures is lower than that of cultures grown on pure methanol (Figs. 2b–4b). This intuitive argument can be made more precise because the threshold specific methanol uptake rate $r_{s,1}^*$ is attained in the dual-limited regime, where $r_{s,1}$ is well-approximated by Eqs. (13)–(14). Hence, the foregoing definition of D^* implies that

$$\frac{D^*}{Y_1}\beta_1(\sigma_1) = r_{s,1}^* \Longrightarrow D^*(\sigma_1) = \frac{Y_1 r_{s,1}^*}{\beta_1(\sigma_1)}. \qquad (15)$$

But Eq. (14) shows that when the fraction of methanol in the feed σ_1 increases from 0 to 1, so does the fraction of biomass derived from methanol β_1. Then Eq. (15) implies that D^* is a decreasing function of σ_1, and therefore achieves its minimum value at $\sigma_1 = 1$ which corresponds to a feed of pure methanol.

3.4 The specific P_{AOX1} expression rate is a function of the specific methanol uptake rate

We have shown above that when the specific methanol uptake rate exceeds the threshold $r_{s,1}^*$, the single- and mixed-substrate cultures yield the same specific P_{AOX1} expression rate. It is relevant to ask if this is true even when the specific methanol uptake rate is below $r_{s,1}^*$. To

this end, the specific LacZ and AOX expression rates $r_{e,1}$ at various D in Figs. 2d–4d were plotted against the corresponding specific methanol uptake rate $r_{s,1}$ in Figs. 2b–4b. This yields the graph in Fig. 5, which shows that the single- and mixed-substrate cultures have the same specific P_{AOX1} expression rates even when the specific methanol uptake rate is below $r_{s,1}^*$, but now the specific P_{AOX1} expression rate is proportional to the specific methanol uptake rate. Thus, to a first approximation, the single- and mixed-substrate specific P_{AOX1} expression rates lie on the graph of the piecewise linear function

$$r_{e,1} = \begin{cases} V_{e,1}\left(\dfrac{r_{s,1}}{r_{s,1}^*}\right), & r_{s,1} \le r_{s,1}^* \\ V_{e,1}, & r_{s,1} > r_{s,1}^* \end{cases}. \qquad (16)$$

The specific P_{AOX1} expression rate is therefore completely determined by the specific methanol uptake rate regardless of the existence (present or absent) and type (repressing or non-repressing) of the secondary carbon source.

3.5 Explaining and predicting the kinetics of recombinant protein production

The data in Fig. 5 explain the observed variation with D of e_1 (Figs. 2c–4c) and $r_{e,1}$ (Figs. 2d–4d). Indeed, if $D \le D^*$, then $r_{s,1} \le r_{s,1}^*$, so that $r_{e,1}$ is proportional to $r_{s,1}$ (Fig. 5) and $r_{s,1}$ is proportional to D (Figs. 2b-4b), which implies that $r_{e,1}$ is proportional to D. Conversely, if $D > D^*$, then $r_{s,1} > r_{s,1}^*$, which implies that $r_{e,1} = V_{e,1}$ (Fig. 5). We can express this argument more precisely by substituting in Eq. (16) the expressions for $r_{s,1}$ and $r_{s,1}^*$ given by Eqs. (13) and (15), thus obtaining the formula

$$r_{e,1} = \begin{cases} V_{e,1}\left(\dfrac{D}{D^*}\right), & D \le D^*, \\ V_{e,1}, & D > D^*. \end{cases} \qquad (17)$$

Then it follows from Eq. (6) that

$$e_1 = \begin{cases} \dfrac{V_{e,1}}{D^*}, & D \le D^*, \\ \dfrac{V_{e,1}}{D}, & D > D^*, \end{cases} \qquad (18)$$

i.e., e_1 is constant up to $D = D^*$, and decreases inversely with D thereafter. Even though Eqs. (17)–(18) have only two parameters, $V_{e,1}$ and D^*, they provide a good fit to the data in Figs.

2c–4c and 2d–4d with the parameter values $V_{e,1} = 4800$ LacZ units mgp^{-1} h^{-1}, $D^* = 0.04$ h^{-1} for pure methanol, and $D^* = 0.06$ h^{-1} for the two mixtures.

The values of $V_{e,1}$ and D^* given above were determined from the extensive data in Fig. 5 and Figs. 2d–4d, but it appears that they can be easily estimated, thus leading to a simple algorithm for predicting the specific protein expression and activity. To see this, observe that $V_{e,1}$ can be estimated from the specific protein activity and maximum specific growth rate during balanced growth on pure methanol in a batch culture; likewise, given the methanol fraction of a feed σ_1, Eq. (15) can be used to estimate $D^*(\sigma_1)$. In principle, substituting these estimates of $V_{e,1}$ and $D^*(\sigma_1)$ in Eqs. (17)–(18) enables prediction of the specific protein expression rate and activity at any D. In practice, this algorithm is likely to work for all cultures fed with methanol and methanol + sorbitol, but not methanol + glycerol. In the latter case, the assumptions underlying Eqs. (17)–(18) are not valid at sufficiently small σ_1 and large D. Indeed, the model assumes that (i) $r_{s,1}$ equals $r_{s,1}^*$ at *some* $D = D^*$, and (ii) $r_{s,1} > r_{s,1}^*$ for *all* $D > D^*$. The first assumption does not hold at sufficiently small σ_1 because under this condition, the specific methanol uptake rate is so low that it does not reach $r_{s,1}^*$ at any D (Egli *et al.,* 1986). The second assumption does not hold at sufficiently large $D > D^*$ because under this condition, the specific methanol uptake rate declines to zero due to glycerol-mediated repression. Further experiments are required to determine the precise bounds on σ_1 and D for which the model is applicable.

3.6 Comparison of recombinant protein production in single- and mixed-substrate cultures

We begin by comparing recombinant protein production on methanol + glycerol and methanol + sorbitol. Several studies have reported that methanol + sorbitol is superior to methanol + glycerol because sorbitol, unlike glycerol, is non-repressing. But in our experiments, both mixtures yielded the same specific activities (Figs. 3c and 4c) and P_{AOX1} expression rates (Figs. 3d and 4d) at every D. We suggest that this is because both mixtures yielded the same specific methanol uptake rates in their dual-limited regimes, which implies that they have the same D^* as well as the same specific P_{AOX1} expression rates for all $D \leq D^*$. To be sure, the specific methanol uptake rates of the two mixtures diverge when $D > D^*$, but since they now exceed the threshold $r_{s,1}^*$, both mixtures still yield the same specific P_{AOX1}

expression rate $V_{e,1}$. Now, Eqs. (13)–(14) imply that given any mixture of methanol + sorbitol, we can always choose a mixture of methanol + glycerol with a value of σ_1 such that both mixtures have the same specific methanol uptake rate in the dual-limited regime. It follows that methanol + sorbitol is not intrinsically superior to methanol + glycerol — the P_{AOX1} expression rates in the two mixtures are determined by the respectivel specific methanol uptake rates, which in turn are determined by the fractions of methanol in the two feeds.

Next, we compare the performance of mixed-substrate cultures with cultures grown on pure methanol. Since the specific methanol uptake rate in mixed-substrate cultures is always lower than that obtained in cultures fed with pure methanol, the specific P_{AOX1} expression rate in mixed-substrate cultures cannot exceed that obtained in cultures limited by pure methanol. To be sure, equality is obtained if D exceeds the D^* for the mixture, but one is unlikely to operate under this condition since it results in suboptimal product yields. If D is lower than the D^* for the mixture, pure methanol provides higher specific expression rates and product yields than those obtained with the mixtures.

4. Discussion

Our main conclusion is that over the range of dilution rates considered in our work (0.02–0.2 h-1), the P_{AOX1} expression rate is completely determined by the methanol uptake rate regardless of the existence and type of the secondary carbon source. This conclusion may appear to subvert the prevailing consensus according to which the expression rate of a promoter is strongly inhibited in the presence of repressing secondary carbon sources. However, we show below that our conclusion is consistent with the chemostat studies reporting the expression of not only the *AOX1* promoter of *K. phaffii* but also the exemplary *lac* promoter of *E. coli*.

4.1 Comparison with chemostat studies of P_{AOX1} expression by *K. phaffii*

von Stockar and co-workers studied the kinetics of biotin expression in Mut^+ cultures during single-substrate growth on glycerol and methanol (Jungo *et al.,* 2006), as well as mixed-substrate growth on methanol + glycerol (Jungo *et al*., 2007a) and methanol + sorbitol (Jungo *et al*., 2007b). Their single-substrate studies, performed by varying D at a fixed feed concentration, are consistent with our results. During growth on glycerol, the specific AOX activity decreased inversely with D. During growth on methanol, the specific AOX activity was

constant up to $D \approx 0.05$ h^{-1}, and decreased inversely with D thereafter, which implies that the specific AOX expression rate increases linearly with D until it saturates beyond the threshold dilution rate of 0.05 h^{-1}; moreover, the corresponding threshold specific methanol uptake rate was 0.15 g gdw^{-1} h^{-1}. The specific biotin expression rates were fitted to linear (Luedeking-Piret) kinetics, $r_{e,1} = \alpha D + \beta$, but a later more extensive study confirmed that biotin expression followed kinetics similar to those shown in Fig. 2d (Schenk et al, 2008).

Jungo *et al* performed their mixed-substrate studies were performed by fixing D, $s_{f,1} + s_{f,2}$ and increasing the fraction of methanol in the feed σ_1 at a slow linear rate aimed at maintaining quasi-steady state. They found that as σ_1 increased:

a) The residual methanol remained negligibly small, and the biomass concentration decreased linearly.
b) The specific biotin expression rate increased hyperbolically until it reached a maximum, which was essentially the same for both mixtures and no different from that obtained with pure methanol.

It follows from a) that the specific methanol uptake rate, which is approximately equal to $D(s_{f,1} + s_{f,2})\sigma_1/x$, increased throughout their experiment. But then b) implies that as the specific methanol uptake rate increased, the specific biotin expression rate of all three cultures reached the *same* maximum (cf. Fig. 5).

Next, we consider the two comparative studies by Berrios and co-workers. In the first study (Canales *et al*., 2015), they compared production of *Rhizopus oryzae* lipase (ROL) by the Mut$^+$ strain during growth on methanol and methanol + glycerol. They found that during growth on methanol, the specific ROL expression rate reached its maximum value at $D = 0.02$ h^{-1}. The very same maximum specific expression rate was also attained during growth on methanol + glycerol, but at the higher dilution rate $D = 0.05$ h^{-1}. Thus, the threshold dilution rate for methanol + glycerol was higher than that for pure methanol. But the threshold specific methanol uptake rate was the same in both cases since the specific methanol uptake rates at $D = 0.02$ h^{-1} on methanol and $D = 0.05$ h^{-1} on methanol + glycerol were essentially the same ($r_{s,1}^* = 0.10$ g gdw^{-1} h^{-1}). This led them to hypothesize that the expression rate was completely determined by the methanol uptake rate regardless of the secondary carbon source. Specifically, they noted that:

"The two distinct feeding strategies (methanol-only and mixed), operated at different conditions, led to similar ROL productivity under similar q_{Meth}. This suggests that the observed effect of q_{Meth} on q_p for mixed feeding (Figure 4a) would be also valid on the induction process with methanol-only feeding. Thus, it would exist a pattern effect of methanol consumption kinetics on ROL q_p regardless of the presence of cosubstrate."

We arrived at the same conclusion based on extensive experimental data obtained in chemostats operated at several dilution rates and fed with not only methanol and methanol + glycerol, but also methanol + sorbitol (Fig. 5). They also observed that during growth on methanol + glycerol, the ROL yield (units $\mathrm{gdw^{-1}}$) decreased monotonically, and hypothesized that, "This effect might be caused by an increase of D rather than the repression by glycerol feeding." This is consistent with our data at large D, where the product yield e_1 is inversely proportional to D, but at small D, which were not considered by Berrios and co-workers, we find that the product yield e_1 is constant (Fig. 3c).

In the second study, Berrios and co-workers compared the methanol uptake and ROL production rates of the $\mathrm{Mut^+}$ strain at two different temperatures (22 and 30 C) during growth on methanol, methanol + glycerol, and methanol + sorbitol (Berrios *et al*., 2016). These experiments were done in chemostats operated at $D = 0.03$ $\mathrm{h^{-1}}$, and in the case of mixed-substrate experiments, fed with two feed compositions (40 and 70 C-mole % methanol). They found that the specific methanol uptake rate during mixed-substrate growth was always less than that observed during single-substrate growth; moreover, the specific ROL expression rate on methanol + glycerol was lower than that observed on pure methanol. Both observations are consistent with our data (Figs. 2b–4b). However, they found that, "Sorbitol-based cultures led to a higher q_p than both glycerol-based and control cultures at most studied conditions." This contradicts our model according to which the specific expression rate of mixed-substrate cultures cannot exceed that observed in methanol-limited cultures. However, closer inspection shows that that in all their experiments, the specific expression rates were 0.8–0.9 units $\mathrm{gdw^{-1}}$ $\mathrm{h^{-1}}$, which is close to the maximum specific expression rate of 1 unit $\mathrm{gdw^{-1}}$ $\mathrm{h^{-1}}$. It is therefore conceivable that the higher productivities observed with sorbitol-based cultures are not statistically significant.

4.2 Comparison with chemostat studies of expression by *lac* promoter of *E. coli*

Analogous results have also been obtained in studies of *lac* expression in *E. coli* Indeed, batch experiments with mixtures of lactose + glycerol, lactose + glucose, and lactose + glucose-6-phophate show that glycerol is non-repressing, whereas glucose and glucose-6-phosphate are repressing (Magasanik, 1970). However, when chemostat experiments were performed with these three mixtures (Smith and Atkinson, 1980), they yielded the *same* steady state specific β-galactosidase (LacZ) activity at all $D \lesssim 0.5$ h^{-1} (Fig. S3). Furthermore, when the steady state specific LacZ activities at various D were plotted against the corresponding specific lactose uptake rates at the same D, the data for all three mixtures collapsed into a single line (Fig. S4). This led the authors to conclude that the steady state specific LacZ activity was "an apparently linear function of the rate of lactose utilization independent of the rate of metabolism of substrates other than lactose which are being concurrently utilized." But then it follows from Eq. (6) that the steady state specific LacZ expression rate is also completely determined by the specific lactose uptake rate regardless of the type (repressing or non-repressing) of the secondary carbon source (Fig. S5).

5. Conclusions

We have shown that the specific P_{AOX1} expression rate is completely determined by the specific methanol uptake rate regardless of the existence (present or absent) and type (repressing or non-repressing) of the secondary carbon source. This result has three important consequences:

1. By combining this functional relation with Egli's unstructured model, which can furnish the specific methanol uptake rate in the dual-limited regime, we can predict the specific protein levels and P_{AOX1} expression rates at the operating conditions typically used for recombinant protein production.
2. Mixtures of methanol + sorbitol are not intrinsically superior to those of methanol + glycerol. By a suitable choice of the fractions of methanol in the two feeds, we can ensure that at every dilution rate, both mixtures exhibit the same specific rates of methanol uptake, and hence, P_{AOX1} expression.

3. The product yields of mixed-substrate cultures can never exceed those attained in cultures grown on pure methanol — in fact, they are strictly lower at the dilution rates typically used for recombinant protein production.
4. Our analysis of the literature shows that the specific expression rate of the *lac* operon of *E. coli* is also completely determined by the specific lactose uptake rate regardless of the type of secondary carbon source.

6. References

Ahmad, M., Hirz, M., Pichler, H., & Schwab, H. 2014. Protein expression in *Pichia pastoris*: recent achievements and perspectives for heterologous protein production. *Applied microbiology and biotechnology*, *98*(12), 5301-5317.

Andrews, J.F., 1968. A mathematical model for the continuous culture of microorganisms utilizing inhibitory substrates. *Biotechnology and bioengineering*, 10(6), pp.707-723.

Arnau, C., Casas, C. and Valero, F., 2011. The effect of glycerol mixed substrate on the heterologous production of a *Rhizopus oryzae* lipase in *Pichia pastoris* system. *Biochemical engineering journal*, *57*, pp.30-37.

Azadi, S., Mahboubi, A., Naghdi, N., Solaimanian, R. and Mortazavi, S.A., 2017. Evaluation of sorbitol-methanol co-feeding strategy on production of recombinant human growth hormone in *Pichia pastoris*. *Iranian journal of pharmaceutical research*: IJPR, *16*(4), p.1555.

Berrios, J., Flores, M.O., Díaz-Barrera, A., Altamirano, C., Martínez, I. and Cabrera, Z., 2017. A comparative study of glycerol and sorbitol as co-substrates in methanol-induced cultures of *Pichia pastoris*: temperature effect and scale-up simulation. *Journal of industrial microbiology & biotechnology*, 44(3), pp.407-411.

Brierley, R. A., Bussineau, C., Kosson, R., Melton, A., & Siegel, R. S. 1990. Fermentation development of recombinant *Pichia pastoris* expressing the heterologous gene: bovine lysozyme. *Annals of the New York Academy of Sciences*, *589*(1), 350-362.

Canales, C., Altamirano, C. and Berrios, J., 2015. Effect of dilution rate and methanol-glycerol mixed feeding on heterologous *Rhizopus oryzae* lipase production with *Pichia pastoris* Mut$^+$ phenotype in continuous culture. Biotechnology Progress, 31(3), pp.707-714.

Carly, F., Niu, H., Delvigne, F. and Fickers, P., 2016. Influence of methanol/sorbitol co-feeding rate on pAOX1 induction in a *Pichia pastoris* Mut$^+$ strain in bioreactor with limited oxygen transfer rate. *Journal of Industrial Microbiology and Biotechnology*, *43*(4), pp.517-523.

Celik, E., Çalık, P. and Oliver, S.G., 2009. Fed-batch methanol feeding strategy for recombinant protein production by *Pichia pastoris* in the presence of co-substrate sorbitol. *Yeast*, *26*(9), pp.473-484.

Chen, L., Mohsin, A., Chu, J., Zhuang, Y., Liu, Y. and Guo, M., 2017. Enhanced protein production by sorbitol co-feeding with methanol in recombinant *Pichia pastoris* strains. *Biotechnology & Bioprocess Engineering*, *22*(6).

Chiruvolu, V., Cregg, J.M. and Meagher, M.M., 1997. Recombinant protein production in an alcohol oxidase-defective strain of *Pichia pastoris* in fed-batch fermentations. *Enzyme and Microbial Technology*, 21(4), pp.277-283.

Cos, O., Ramón, R., Montesinos, J.L. and Valero, F., 2006. Operational strategies, monitoring and control of heterologous protein production in the methylotrophic yeast *Pichia pastoris* under different promoters: a review. *Microbial cell factories*, *5*(1), pp.1-20.

Cregg, J.M., Barringer, K.J., Hessler, A.Y. and Madden, K.R., 1985. *Pichia pastoris* as a host system for transformations. *Molecular and cellular biology*, 5(12), pp.3376-3385.

Cregg, J.M., Madden, K.R., Barringer, K.J., Thill, G.P. and Stillman, C.A., 1989. Functional characterization of the two alcohol oxidase genes from the yeast *Pichia pastoris*. *Molecular and cellular biology*, 9(3), pp.1316-1323.

Egli, T. and Fiechter, A., 1981. Theoretical analysis of media used in the growth of yeasts on methanol. *Microbiology*, 123(2), pp.365-369.

Egli, T., Bosshard, C., & Hamer, G. 1986. Simultaneous utilization of methanol–glucose mixtures by *Hansenula polymorpha* in chemostat: Influence of dilution rate and mixture composition on utilization pattern. *Biotechnology and bioengineering*, *28*(11), 1735-1741.

Egli, T., Käppeli, O., & Fiechter, A. 1982. Regulatory flexibility of methylotrophic yeasts in chemostat cultures: simultaneous assimilation of glucose and methanol at a fixed dilution rate. *Archives of Microbiology*, *131*(1), 1-7.

Gao, M.J., Li, Z., Yu, R.S., Wu, J.R., Zheng, Z.Y., Shi, Z.P., Zhan, X.B. and Lin, C.C., 2012. Methanol/sorbitol co-feeding induction enhanced porcine interferon-α production by *P. pastoris* associated with energy metabolism shift. *Bioprocess and biosystems engineering*, *35*(7), pp.1125-1136.

García-Ortega, X., Cámara, E., Ferrer, P., Albiol, J., Montesinos-Seguí, J.L. and Valero, F., 2019. Rational development of bioprocess engineering strategies for recombinant protein

production in *Pichia pastoris* (*Komagataella phaffii*) using the methanol-free GAP promoter. Where do we stand?. *New biotechnology*, *53*, pp.24-34.

Gasser, B., & Mattanovich, D. 2018. A yeast for all seasons–Is *Pichia pastoris* a suitable chassis organism for future bioproduction?. *FEMS microbiology letters*, *365*(17), fny181.

Higgins, D.R. and Cregg, J.M., 1998. Introduction to *Pichia pastoris*. In *Pichia protocols* (pp. 1-15). Humana Press.

Inan, M., & Meagher, M. M. 2001. Non-repressing carbon sources for alcohol oxidase (AOX1) promoter of *Pichia pastoris*. *Journal of Bioscience and Bioengineering*, *92*(6), 585-589.

Jahic, M., Veide, A., Charoenrat, T., Teeri, T. and Enfors, S.O., 2006. Process technology for production and recovery of heterologous proteins with *Pichia pastoris*. *Biotechnology progress*, *22*(6), pp.1465-1473.

Jungo, C., Marison, I., & von Stockar, U. 2007a. Mixed feeds of glycerol and methanol can improve the performance of *Pichia pastoris* cultures: A quantitative study based on concentration gradients in transient continuous cultures. *Journal of biotechnology*, *128*(4), 824-837.

Jungo, C., Rérat, C., Marison, I.W. and von Stockar, U., 2006. Quantitative characterization of the regulation of the synthesis of alcohol oxidase and of the expression of recombinant avidin in a *Pichia pastoris* Mut$^+$ strain. *Enzyme and microbial technology*, *39*(4), pp.936-944.

Jungo, C., Schenk, J., Pasquier, M., Marison, I. W., & von Stockar, U. 2007b. A quantitative analysis of the benefits of mixed feeds of sorbitol and methanol for the production of recombinant avidin with *Pichia pastoris*. *Journal of biotechnology*, *131*(1), 57-66.

Juturu, V. and Wu, J.C., 2018. Heterologous protein expression in *Pichia pastoris*: latest research progress and applications. *ChemBioChem*, *19*(1), pp.7-21.

Lendenmann, U. R. S., Snozzi, M., & Egli, T. 1996. Kinetics of the simultaneous utilization of sugar mixtures by *Escherichia coli* in continuous culture. *Applied and Environmental Microbiology*, *62*(5), 1493-1499.

Liu, W.C., Inwood, S., Gong, T., Sharma, A., Yu, L.Y. and Zhu, P., 2019. Fed-batch high-cell-density fermentation strategies for *Pichia pastoris* growth and production. *Critical reviews in biotechnology*, *39*(2), pp.258-271.

Macauley-Patrick, S., Fazenda, M.L., McNeil, B. and Harvey, L.M., 2005. Heterologous protein production using the *Pichia pastoris* expression system. *Yeast*, *22*(4), pp.249-270.

Magasanik, B. 1970. Glucose effects: inducer exclusion and repression. In:The Lactose Operon (eds J. Beckwith & D. Zipser), pp. 189–220. Cold Spring Harbor, NY: Cold Spring Harbor Laboratory Press.

Nieto-Taype, M.A., Garcia-Ortega, X., Albiol, J., Montesinos-Seguí, J.L. and Valero, F., 2020. Continuous cultivation as a tool toward the rational bioprocess development with *Pichia Pastoris* cell factory. *Frontiers in Bioengineering and Biotechnology*, *8*, p.632.

Niu, H., Jost, L., Pirlot, N., Sassi, H., Daukandt, M., Rodriguez, C. and Fickers, P., 2013. A quantitative study of methanol/sorbitol co-feeding process of a *Pichia pastoris* Mut$^+$/pAOX1-lacZ strain. *Microbial cell factories*, *12*(1), pp.1-8.

Noel, J.T. and Narang, A., 2009. Gene regulation in continuous cultures: A unified theory for bacteria and yeasts. *Bulletin of mathematical biology*, *71*(2), pp.453-514.

Paulová, L., Hyka, P., Branská, B., Melzoch, K., & Kovar, K. 2012. Use of a mixture of glucose and methanol as substrates for the production of recombinant trypsinogen in continuous cultures with *Pichia pastoris* Mut$^+$. *Journal of biotechnology*, *157*(1), 180-188.

Pirt, S.J., 1965. The maintenance energy of bacteria in growing cultures. *Proceedings of the Royal Society of London. Series B. Biological Sciences*, *163*(991), pp.224-231.

Potvin, G., Ahmad, A. and Zhang, Z., 2012. Bioprocess engineering aspects of heterologous protein production in *Pichia pastoris*: a review. *Biochemical Engineering Journal*, *64*, pp.91-105.

Ramón, R., Ferrer, P. and Valero, F., 2007. Sorbitol co-feeding reduces metabolic burden caused by the overexpression of a *Rhizopus oryzae* lipase in *Pichia pastoris*. *Journal of Biotechnology*, *130*(1), pp.39-46.

Schenk, J., Balazs, K., Jungo, C., Urfer, J., Wegmann, C., Zocchi, A., Marison, I.W. and von Stockar, U., 2008. Influence of specific growth rate on specific productivity and glycosylation of a recombinant avidin produced by a *Pichia pastoris* Mut^+ strain. *Biotechnology and bioengineering*, *99*(2), pp.368-377.

Schwarzhans, J.P., Wibberg, D., Winkler, A., Luttermann, T., Kalinowski, J. and Friehs, K., 2016. Non-canonical integration events in *Pichia pastoris* encountered during standard transformation analysed with genome sequencing. *Scientific reports*, 6, p.38952.

Singh, A., & Narang, A. 2020. The Mut+ strain of *Komagataella phaffii* (*Pichia pastoris*) expresses P_{AOX1} 5- and 10-times faster than Mut^s and Mut^- strains: evidence that formaldehyde or/and formate are true inducers of P_{AOX1}. *Applied Microbiology and Biotechnology*, *104*(18), 7801-7814.

Smith, S. S., & Atkinson, D. E. 1980. The expression of β-galactosidase by *Escherichia coli* during continuous culture. *Archives of biochemistry and biophysics*, *202*(2), 573-581.

Sreekrishna, K., Brankamp, R. G., Kropp, K. E., Blankenship, D. T., Tsay, J. T., Smith, P. L., ... & Birkenberger, L. A. 1997. Strategies for optimal synthesis and secretion of heterologous proteins in the methylotrophic yeast *Pichia pastoris*. *Gene*, *190*(1), 55-62.

Thorpe, E. D., d'Anjou, M. C., & Daugulis, A. J. 1999. Sorbitol as a non-repressing carbon source for fed-batch fermentation of recombinant *Pichia pastoris*. *Biotechnology letters*, *21*(8), 669-672.

Wang, Z., Wang, Y., Zhang, D., Li, J., Hua, Z., Du, G. and Chen, J., 2010. Enhancement of cell viability and alkaline polygalacturonate lyase production by sorbitol co-feeding with methanol in Pichia pastoris fermentation. *Bioresource technology*, *101*(4), pp.1318-1323.

Xie, J., Zhou, Q., Du, P., Gan, R., & Ye, Q. 2005. Use of different carbon sources in cultivation of recombinant *Pichia pastoris* for angiostatin production. *Enzyme and Microbial Technology*, *36*(2-3), 210-216.

Yang, Z. and Zhang, Z., 2018. Engineering strategies for enhanced production of protein and bio-products in *Pichia pastoris*: a review. *Biotechnology advances*, *36*(1), pp.182-195.

Table 1: Maximum specific growth rates and biomass yields during single-substrate growth of the Mut$^+$ strain of *K. phaffii* on glycerol, sorbitol, and methanol. The true biomass yield in the chemostat was determined by fitting the variation of the specific substrate uptake rate with D to Pirt's model.

Carbon source	Maximum specific growth rate (h^{-1})	Biomass yield in shake flask (gdw g^{-1})	True biomass yield in chemostat (gdw g^{-1})
Glycerol	0.24 ± 0.01	0.61 ± 0.03	0.67
Sorbitol	0.03 ± 0.01	0.56 ± 0.01	ND
Methanol	0.11 ± 0.01	0.29 ± 0.01	0.27

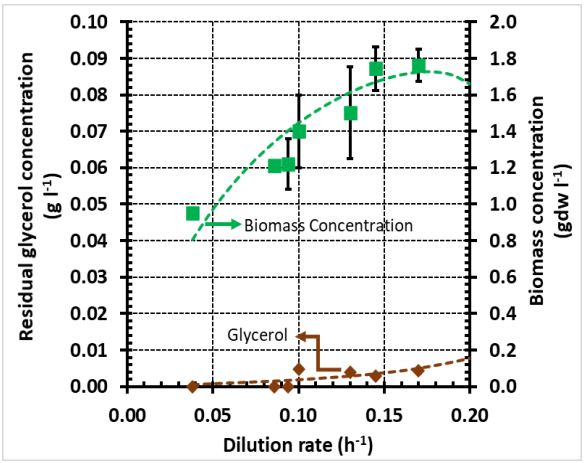

(a)

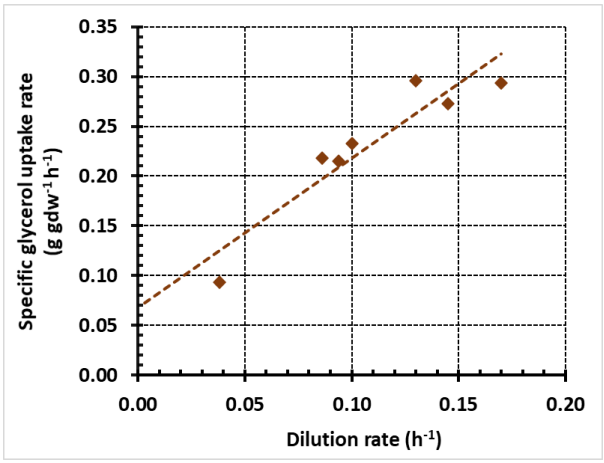

(b)

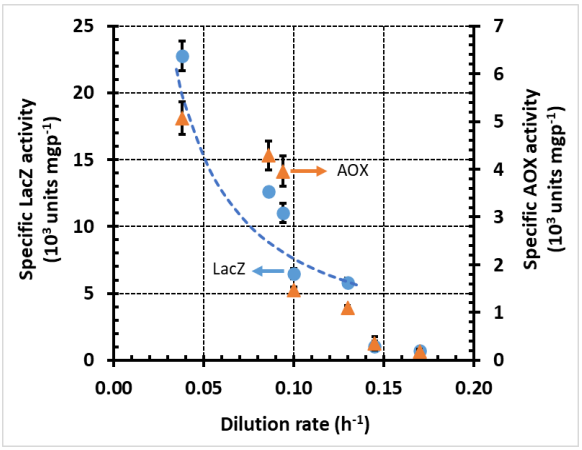

(c)

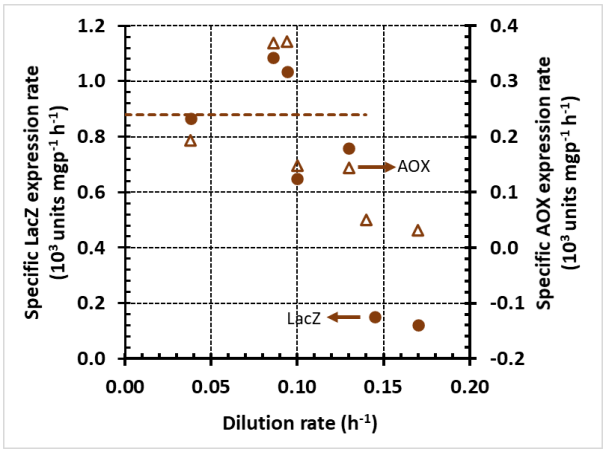

(d)

Fig. 1: Variation of steady state concentrations and rates with the dilution rate during growth of *K. phaffii* strain Mut$^+$ (pSAOH5-T1) in a chemostat fed with glycerol (~3.1 g l^{-1}). (a) Concentrations of biomass and residual glycerol. (b) Specific glycerol uptake rates calculated from the data in (a) using Eq. (5). (c) Specific activities of LacZ and AOX. (d) Specific Lac Z and AOX expression rates calculated from the data in (c) using Eq. (6).

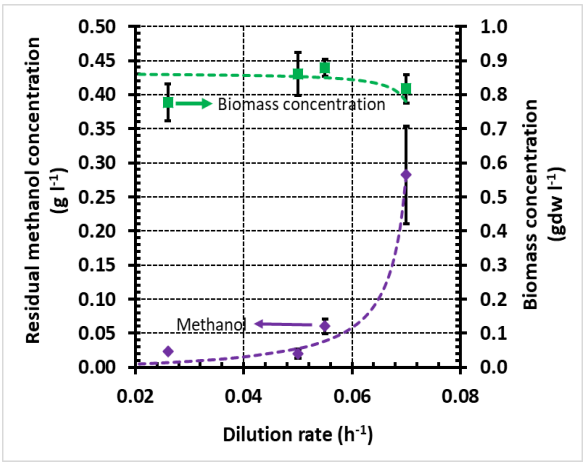

(a)

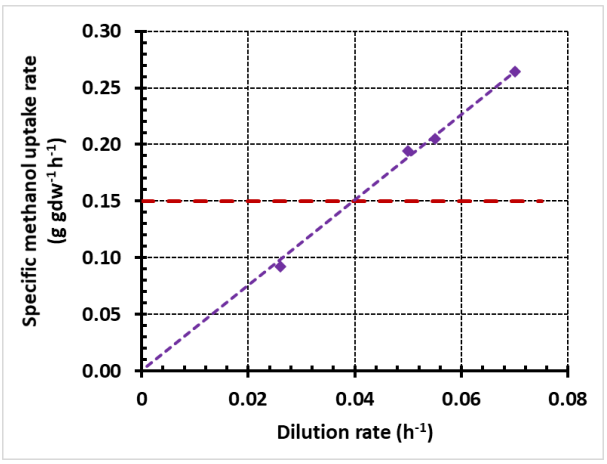

(b)

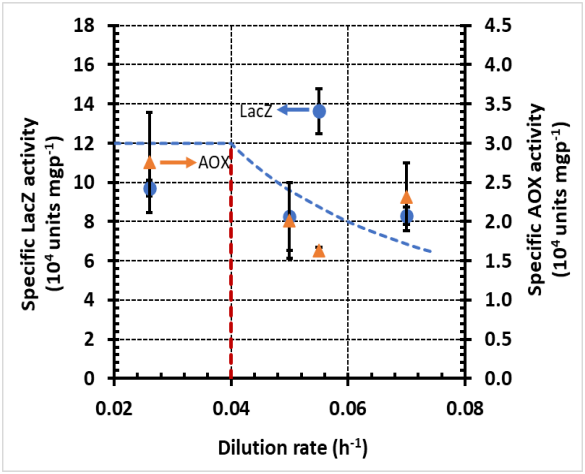

(c)

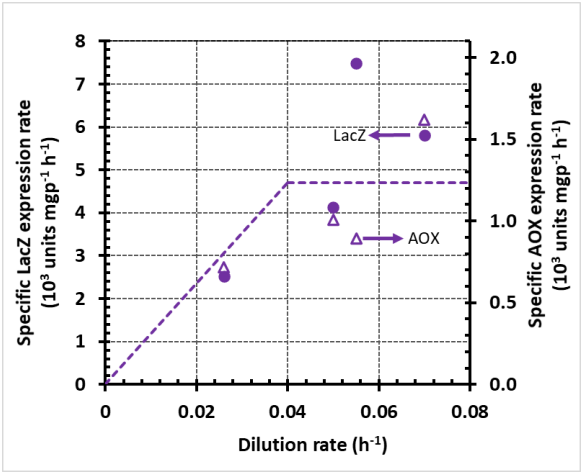

(d)

Fig. 2: Variation of steady state concentrations and rates with the dilution rate during growth of *K. phaffii* strain Mut$^+$ (pSAOH5-T1) in a chemostat fed with methanol (~3.2 g l^{-1}). (a) Concentrations of biomass and residual methanol. (b) Specific methanol uptake rates calculated from the data in (a) using Eq. (5). The horizontal dashed line shows the threshold specific methanol uptake rate of 0.15 g gdw^{-1} h^{-1}. (c) Specific LacZ and AOX activities. The data were fitted using Eq. (18). (d) Specific LacZ and AOX expression rates calculated from the data in (c) using Eq. (6). The data were fitted using Eq. (17).

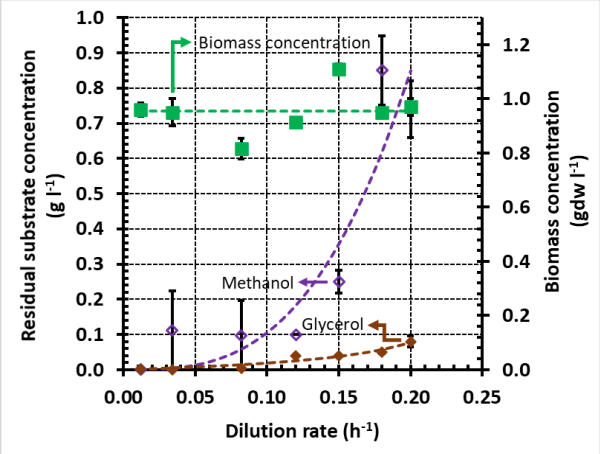

(a)

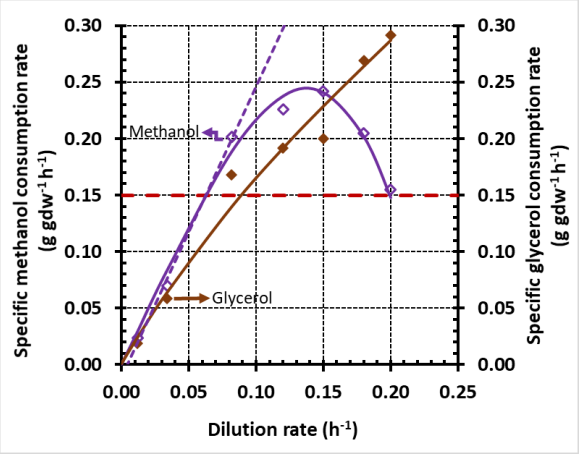

(b)

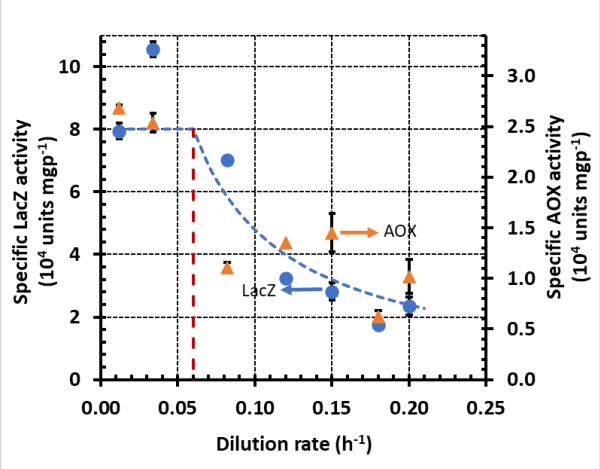

(c)

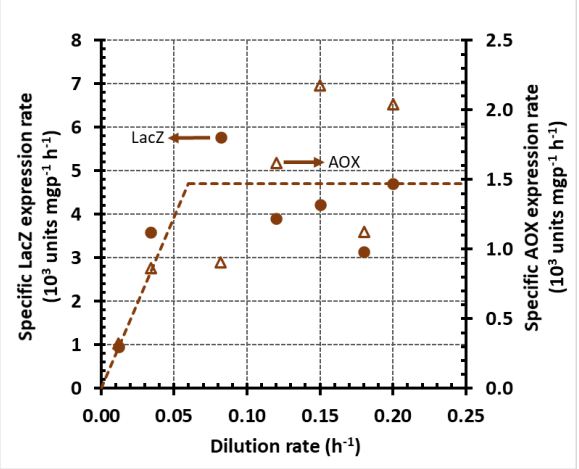

(d)

Fig. 3: Variation of steady state concentrations with the dilution rate during growth of *K. phaffii* strain Mut$^+$ (pSAOH5-T1) in a chemostat fed with a mixture of glycerol (~1.5 g l^{-1}) and methanol ~(1.6 g l^{-1}). (a) Concentrations of biomass, residual glycerol, and residual methanol (b) Specific methanol and glycerol uptake rates calculated from the data in (a) using Eq. (5). The dashed line passing through the origin shows the specific methanol uptake estimated from Eqs. (13)-(14). The horizontal dashed line shows the threshold specific methanol uptake rate of 0.15 g gdw^{-1} h^{-1}. (c) Specific activities of LacZ and AOX. The data were fitted using Eq. (18). (d) Specific LacZ and AOX expression rates calculated from the data in (c) using Eq. (6). The data were fitted using Eq. (17).

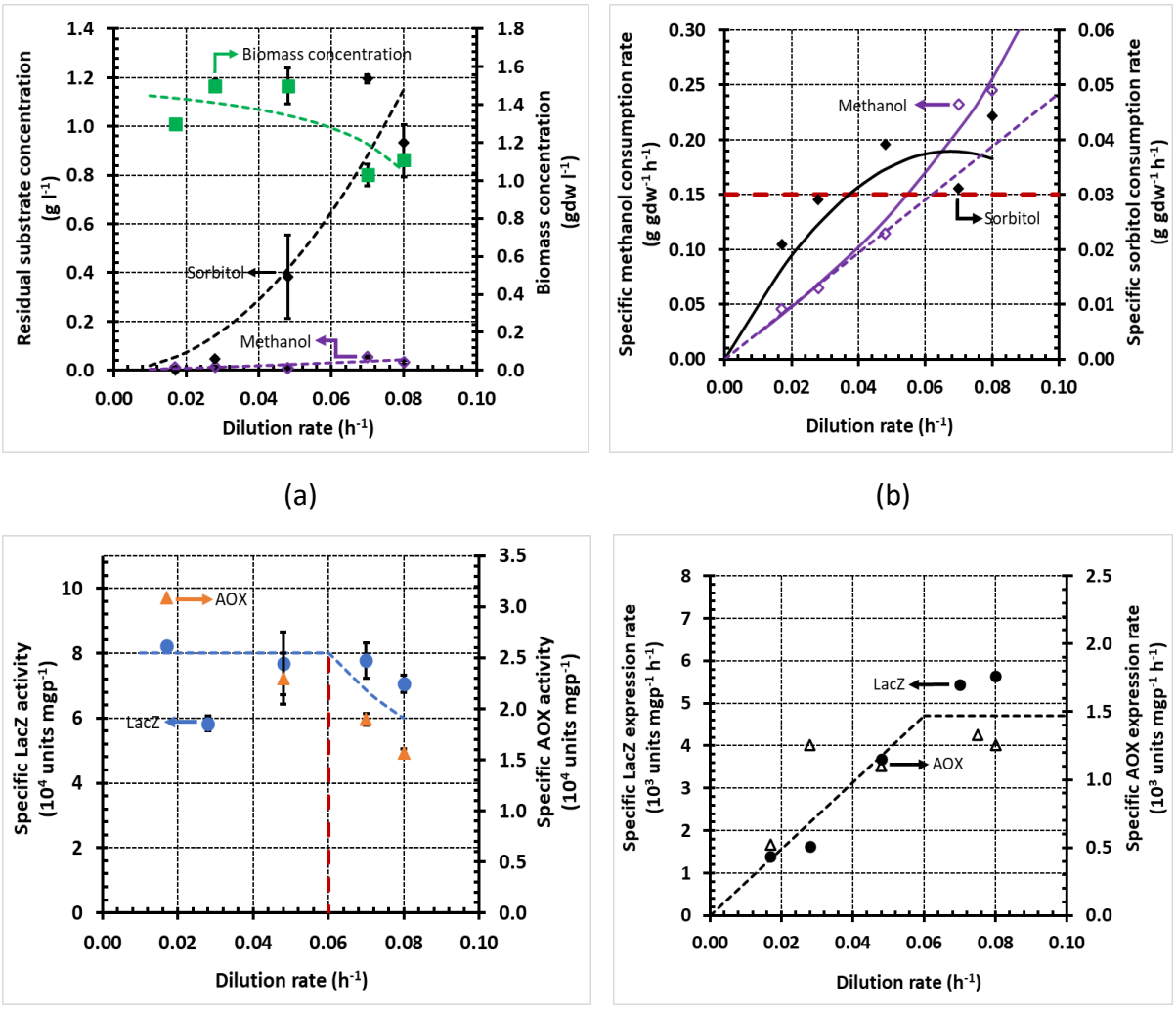

Fig. 4: Variation of steady state concentrations with the dilution rate during growth of *K. phaffii* strain Mut$^+$ (pSAOH5-T1) in a chemostat fed with a mixture of sorbitol (~1.5 g l^{-1}) and methanol (~3.2 g l^{-1}). (a) Concentrations of biomass, residual sorbitol and residual methanol. (b) Specific methanol and glycerol uptake rates calculated from the data in (a) using Eq. (5). The dashed line passing through the origin shows the specific methanol uptake estimated from Eqs. (13)-(14). The horizontal dashed line shows the threshold specific methanol uptake rate of 0.15 g gdw^{-1} h^{-1}. (c) Specific activities of LacZ and AOX. The data were fitted using Eq. (18). (d) Specific LacZ and AOX expression rates calculated from the data in (c) using Eq. (6). The data were fitted using Eq. (17).

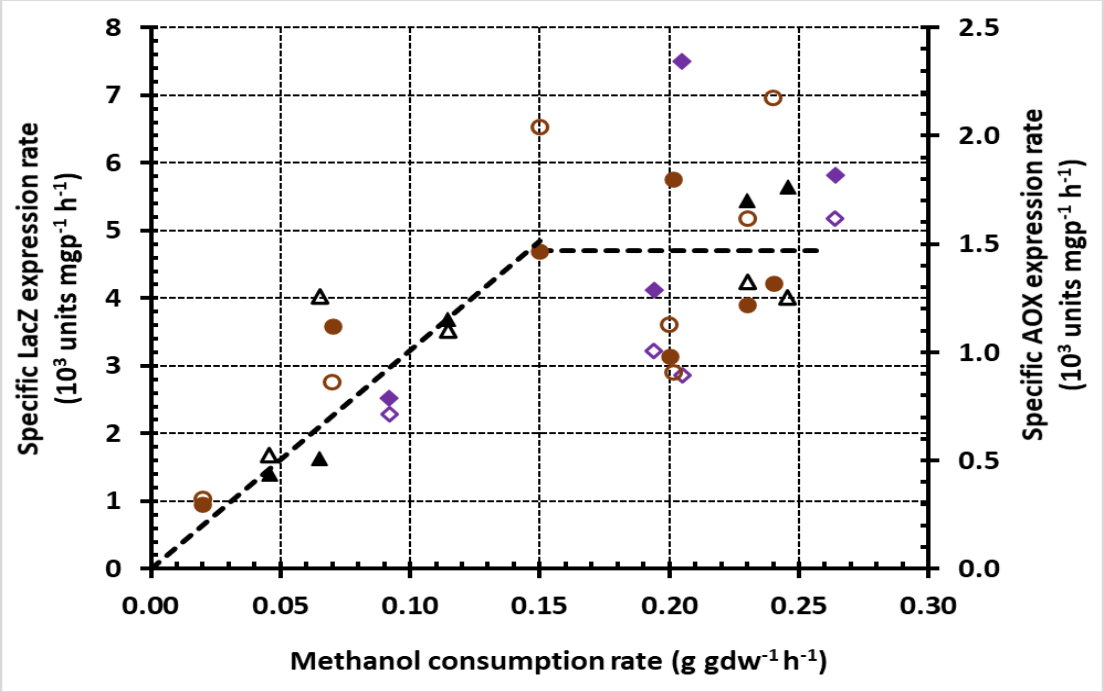

Fig. 5: Variation of the specific LacZ (closed circles) and AOX (open triangles) expression rates with the specific methanol uptake rate during growth on methanol (purple) methanol + glycerol (brown) and methanol + sorbitol (black) The graph was obtained by plotting the specific methanol consumption rates in Figs. 2b–4b against the corresponding specific LacZ and AOX expression rates in Figs. 2d–4d. The dashed line shows the fit to the data obtained using Eq. (15) with the threshold specific methanol uptake rate $r_{s,1}^{*} = 0.15$ g h^{-1} gdw^{-1} and the maximum specific LacZ expression rate $V_{e,1} = 4800$ units mgp^{-1} h^{-1}.